Dijet Mass Spectrum and a Search for Quark Compositeness in $\overline{p}p$ Collisions at $\sqrt{s} = 1.8$ TeV

B. Abbott,[40] M. Abolins,[37] V. Abramov,[15] B. S. Acharya,[8] I. Adam,[39] D. L. Adams,[48] M. Adams,[24] S. Ahn,[23] H. Aihara,[17] G. A. Alves,[2] N. Amos,[36] E. W. Anderson,[30] R. Astur,[42] M. M. Baarmand,[42] V. V. Babintsev,[15] L. Babukhadia,[16] A. Baden,[33] V. Balamurali,[28] B. Baldin,[23] S. Banerjee,[8] J. Bantly,[45] E. Barberis,[17] P. Baringer,[31] J. F. Bartlett,[23] A. Belyaev,[14] S. B. Beri,[6] I. Bertram,[26] V. A. Bezzubov,[15] P. C. Bhat,[23] V. Bhatnagar,[6] M. Bhattacharjee,[42] N. Biswas,[28] G. Blazey,[25] S. Blessing,[21] P. Bloom,[18] A. Boehnlein,[23] N. I. Bojko,[15] F. Borcherding,[23] C. Boswell,[20] A. Brandt,[23] R. Breedon,[18] R. Brock,[37] A. Bross,[23] D. Buchholz,[26] V. S. Burtovoi,[15] J. M. Butler,[34] W. Carvalho,[2] D. Casey,[37] Z. Casilum,[42] H. Castilla-Valdez,[11] D. Chakraborty,[42] S.-M. Chang,[35] S. V. Chekulaev,[15] L.-P. Chen,[17] W. Chen,[42] S. Choi,[10] S. Chopra,[36] B. C. Choudhary,[20] J. H. Christenson,[23] M. Chung,[24] D. Claes,[38] A. R. Clark,[17] W. G. Cobau,[33] J. Cochran,[20] L. Coney,[28] W. E. Cooper,[23] C. Cretsinger,[41] D. Cullen-Vidal,[45] M. A. C. Cummings,[25] D. Cutts,[45] O. I. Dahl,[17] K. Davis,[16] K. De,[46] K. Del Signore,[36] M. Demarteau,[23] D. Denisov,[23] S. P. Denisov,[15] H. T. Diehl,[23] M. Diesburg,[23] G. Di Loreto,[37] P. Draper,[46] Y. Ducros,[5] L. V. Dudko,[14] S. R. Dugad,[8] A. Dyshkant,[15] D. Edmunds,[37] J. Ellison,[20] V. D. Elvira,[42] R. Engelmann,[42] S. Eno,[33] G. Eppley,[48] P. Ermolov,[14] O. V. Eroshin,[15] V. N. Evdokimov,[15] T. Fahland,[19] M. K. Fatyga,[41] S. Feher,[23] D. Fein,[16] T. Ferbel,[41] G. Finocchiaro,[42] H. E. Fisk,[23] Y. Fisyak,[43] E. Flattum,[23] G. E. Forden,[16] M. Fortner,[25] K. C. Frame,[37] S. Fuess,[23] E. Gallas,[46] A. N. Galyaev,[15] P. Gartung,[20] V. Gavrilov,[13] T. L. Geld,[37] R. J. Genik II,[37] K. Genser,[23] C. E. Gerber,[23] Y. Gershtein,[13] B. Gibbard,[43] B. Gobbi,[26] B. Gómez,[4] G. Gómez,[33] P. I. Goncharov,[15] J. L. González Solís,[11] H. Gordon,[43] L. T. Goss,[47] K. Gounder,[20] A. Goussiou,[42] N. Graf,[43] P. D. Grannis,[42] D. R. Green,[23] H. Greenlee,[23] S. Grinstein,[1] P. Grudberg,[17] S. Grünendahl,[23] G. Guglielmo,[44] J. A. Guida,[16] J. M. Guida,[45] A. Gupta,[8] S. N. Gurzhiev,[15] G. Gutierrez,[23] P. Gutierrez,[44] N. J. Hadley,[33] H. Haggerty,[23] S. Hagopian,[21] V. Hagopian,[21] K. S. Hahn,[41] R. E. Hall,[19] P. Hanlet,[35] S. Hansen,[23] J. M. Hauptman,[30] D. Hedin,[25] A. P. Heinson,[20] U. Heintz,[23] R. Hernández-Montoya,[11] T. Heuring,[21] R. Hirosky,[24] J. D. Hobbs,[42] B. Hoeneisen,[4,*] J. S. Hoftun,[45] F. Hsieh,[36] Ting Hu,[42] Tong Hu,[27] T. Huehn,[20] A. S. Ito,[23] E. James,[16] J. Jaques,[28] S. A. Jerger,[37] R. Jesik,[27] T. Joffe-Minor,[26] K. Johns,[16] M. Johnson,[23] A. Jonckheere,[23] M. Jones,[22] H. Jöstlein,[23] S. Y. Jun,[26] C. K. Jung,[42] S. Kahn,[43] G. Kalbfleisch,[44] D. Karmanov,[14] D. Karmgard,[21] R. Kehoe,[28] M. L. Kelly,[28] S. K. Kim,[10] B. Klima,[23] C. Klopfenstein,[18] W. Ko,[18] J. M. Kohli,[6] D. Koltick,[29] A. V. Kostritskiy,[15] J. Kotcher,[43] A. V. Kotwal,[39] A. V. Kozelov,[15] E. A. Kozlovsky,[15] J. Krane,[38] M. R. Krishnaswamy,[8] S. Krzywdzinski,[23] S. Kuleshov,[13] S. Kunori,[33] F. Landry,[37] G. Landsberg,[45] B. Lauer,[30] A. Leflat,[14] J. Li,[46] Q. Z. Li-Demarteau,[23] J. G. R. Lima,[23] D. Lincoln,[23] S. L. Linn,[21] J. Linnemann,[37] R. Lipton,[23] F. Lobkowicz,[41] S. C. Loken,[17] A. Lucotte,[42] L. Lueking,[23] A. L. Lyon,[23] A. K. A. Maciel,[2] R. J. Madaras,[17] R. Madden,[21] L. Magaña-Mendoza,[11] V. Manankov,[14] S. Mani,[18] H. S. Mao,[23,†] R. Markeloff,[25] T. Marshall,[27] M. I. Martin,[23] K. M. Mauritz,[30] B. May,[26] A. A. Mayorov,[15] R. McCarthy,[42] J. McDonald,[21] T. McKibben,[24] J. McKinley,[37] T. McMahon,[44] H. L. Melanson,[23] M. Merkin,[14] K. W. Merritt,[23] C. Miao,[45] H. Miettinen,[48] A. Mincer,[40] C. S. Mishra,[23] N. Mokhov,[23] N. K. Mondal,[8] H. E. Montgomery,[23] P. Mooney,[4] M. Mostafa,[1] H. da Motta,[2] C. Murphy,[24] F. Nang,[16] M. Narain,[23] V. S. Narasimham,[8] A. Narayanan,[16] H. A. Neal,[36] J. P. Negret,[4] P. Nemethy,[40] D. Norman,[47] L. Oesch,[36] V. Oguri,[3] E. Oliveira,[2] E. Oltman,[17] N. Oshima,[23] D. Owen,[37] P. Padley,[48] A. Para,[23] Y. M. Park,[9] R. Partridge,[45] N. Parua,[8] M. Paterno,[41] B. Pawlik,[12] J. Perkins,[46] M. Peters,[22] R. Piegaia,[1] H. Piekarz,[21] Y. Pischalnikov,[29] B. G. Pope,[37] H. B. Prosper,[21] S. Protopopescu,[43] J. Qian,[36] P. Z. Quintas,[23] R. Raja,[23] S. Rajagopalan,[43] O. Ramirez,[24] S. Reucroft,[35] M. Rijssenbeek,[42] T. Rockwell,[37] M. Roco,[23] P. Rubinov,[26] R. Ruchti,[28] J. Rutherfoord,[16] A. Sánchez-Hernández,[11] A. Santoro,[2] L. Sawyer,[32] R. D. Schamberger,[42] H. Schellman,[26] J. Sculli,[40] E. Shabalina,[14] C. Shaffer,[21] H. C. Shankar,[8] R. K. Shivpuri,[7] M. Shupe,[16] H. Singh,[20] J. B. Singh,[6] V. Sirotenko,[25] E. Smith,[44] R. P. Smith,[23] R. Snihur,[26] G. R. Snow,[38] J. Snow,[44] S. Snyder,[43] J. Solomon,[24] M. Sosebee,[46] N. Sotnikova,[14] M. Souza,[2] A. L. Spadafora,[17] G. Steinbrück,[44] R. W. Stephens,[46] M. L. Stevenson,[17] D. Stewart,[36] F. Stichelbaut,[42] D. Stoker,[19] V. Stolin,[13] D. A. Stoyanova,[15] M. Strauss,[44] K. Streets,[40] M. Strovink,[17] A. Sznajder,[2] P. Tamburello,[33] J. Tarazi,[19] M. Tartaglia,[23] T. L. T. Thomas,[26] J. Thompson,[33] T. G. Trippe,[17] P. M. Tuts,[39] V. Vaniev,[15] N. Varelas,[24] E. W. Varnes,[17] D. Vititoe,[16] A. A. Volkov,[15] A. P. Vorobiev,[15] H. D. Wahl,[21] G. Wang,[21] J. Warchol,[28] G. Watts,[45] M. Wayne,[28] H. Weerts,[37] A. White,[46] J. T. White,[47] J. A. Wightman,[30] S. Willis,[25] S. J. Wimpenny,[20] J. V. D. Wirjawan,[47] J. Womersley,[23] E. Won,[41] D. R. Wood,[35] Z. Wu,[23,†] H. Xu,[45] R. Yamada,[23] P. Yamin,[43] T. Yasuda,[35] P. Yepes,[48] K. Yip,[23] C. Yoshikawa,[22] S. Youssef,[21] J. Yu,[23] Y. Yu,[10]

0031-9007/99/82(12)/2457(6)$15.00

B. Zhang,[23,†] Y. Zhou,[23,†] Z. Zhou,[30] Z. H. Zhu,[41] M. Zielinski,[41] D. Zieminska,[27] A. Zieminski,[27] E. G. Zverev,[14] and A. Zylberstejn[5]

(D0 Collaboration)

[1]*Universidad de Buenos Aires, Buenos Aires, Argentina*
[2]*LAFEX, Centro Brasileiro de Pesquisas Físicas, Rio de Janeiro, Brazil*
[3]*Universidade do Estado do Rio de Janeiro, Rio de Janeiro, Brazil*
[4]*Universidad de los Andes, Bogotá, Colombia*
[5]*DAPNIA/Service de Physique des Particules, CEA, Saclay, France*
[6]*Panjab University, Chandigarh, India*
[7]*Delhi University, Delhi, India*
[8]*Tata Institute of Fundamental Research, Mumbai, India*
[9]*Kyungsung University, Pusan, Korea*
[10]*Seoul National University, Seoul, Korea*
[11]*CINVESTAV, Mexico City, Mexico*
[12]*Institute of Nuclear Physics, Kraków, Poland*
[13]*Institute for Theoretical and Experimental Physics, Moscow, Russia*
[14]*Moscow State University, Moscow, Russia*
[15]*Institute for High Energy Physics, Protvino, Russia*
[16]*University of Arizona, Tucson, Arizona 85721*
[17]*Lawrence Berkeley National Laboratory and University of California, Berkeley, California 94720*
[18]*University of California, Davis, California 95616*
[19]*University of California, Irvine, California 92697*
[20]*University of California, Riverside, California 92521*
[21]*Florida State University, Tallahassee, Florida 32306*
[22]*University of Hawaii, Honolulu, Hawaii 96822*
[23]*Fermi National Accelerator Laboratory, Batavia, Illinois 60510*
[24]*University of Illinois at Chicago, Chicago, Illinois 60607*
[25]*Northern Illinois University, DeKalb, Illinois 60115*
[26]*Northwestern University, Evanston, Illinois 60208*
[27]*Indiana University, Bloomington, Indiana 47405*
[28]*University of Notre Dame, Notre Dame, Indiana 46556*
[29]*Purdue University, West Lafayette, Indiana 47907*
[30]*Iowa State University, Ames, Iowa 50011*
[31]*University of Kansas, Lawrence, Kansas 66045*
[32]*Louisiana Tech University, Ruston, Louisiana 71272*
[33]*University of Maryland, College Park, Maryland 20742*
[34]*Boston University, Boston, Massachusetts 02215*
[35]*Northeastern University, Boston, Massachusetts 02115*
[36]*University of Michigan, Ann Arbor, Michigan 48109*
[37]*Michigan State University, East Lansing, Michigan 48824*
[38]*University of Nebraska, Lincoln, Nebraska 68588*
[39]*Columbia University, New York, New York 10027*
[40]*New York University, New York, New York 10003*
[41]*University of Rochester, Rochester, New York 14627*
[42]*State University of New York, Stony Brook, New York 11794*
[43]*Brookhaven National Laboratory, Upton, New York 11973*
[44]*University of Oklahoma, Norman, Oklahoma 73019*
[45]*Brown University, Providence, Rhode Island 02912*
[46]*University of Texas, Arlington, Texas 76019*
[47]*Texas A&M University, College Station, Texas 77843*
[48]*Rice University, Houston, Texas 77005*

(Received 16 July 1998)

Using the D0 detector at the 1.8 TeV $\overline{p}p$ Fermilab Tevatron collider, we have measured the inclusive dijet mass spectrum in the central pseudorapidity region $|\eta_{\text{jet}}| < 1.0$ for dijet masses greater than 200 GeV/c^2. We have also measured the ratio of spectra $\sigma(|\eta_{\text{jet}}| < 0.5)/\sigma(0.5 < |\eta_{\text{jet}}| < 1.0)$. The order α_s^3 quantum chromodynamics predictions are in good agreement with the data and we rule out models of quark compositeness with a contact interaction scale <2.4 TeV at the 95% confidence level. [S0031-9007(99)08799-2]

PACS numbers: 13.87.Ce, 12.38.Qk, 12.60.Rc, 13.85.Ni

High transverse energy (E_T) jet production at a center of mass energy of 1.8 TeV probes the structure of the proton down to a distance scale of 10^{-4} fm. A measurement of the dijet mass spectrum can be used to verify the predictions of quantum chromodynamics (QCD) for parton-parton scattering and to constrain the parton distribution functions (pdf) of the proton. Additionally, new physics such as quark compositeness [1] would be revealed by an excess of events in the dijet mass (M) spectrum at high masses with respect to the predictions of QCD. A previous analysis by the CDF collaboration of the inclusive jet cross section [2] reported an excess of jet production at high E_T. More recent analyses of the dijet angular distribution by D0 [3] and CDF [4] have excluded, at the 95% confidence level, models of quark compositeness in which the contact interaction scale is below 2 TeV. Most recently, an analysis of the inclusive jet cross section by D0 [5] shows good agreement between the theory and data. This paper presents a new improved measurement by D0 of the inclusive dijet mass (M) spectrum (uncertainty reduced by a factor of 4 at $M = 200$ GeV/c^2 relative to the previous CDF measurement [6]) and improved limits on the contact interaction scale.

The outgoing partons from the parton-parton scattering process hadronize to form jets of particles. These jets were identified in the D0 detector [7] using uranium/liquid-argon calorimeters which cover a pseudorapidity range of $|\eta| \leq 4.1$ ($\eta = -\ln[\tan(\theta/2)]$, where θ is the polar angle).

Events with at least one inelastic interaction during a beam crossing were identified using scintillator hodoscopes, and the primary event vertex was determined using tracks reconstructed in the central tracking system. Event selection occurred in two stages. A minimum transverse energy was required in a region ($\Delta\eta \times \Delta\phi = 0.8 \times 1.6$) of the calorimeter. Jet candidates were then reconstructed online with a cone algorithm of opening angle $\mathcal{R} = 0.7$ in η-ϕ space (ϕ is the azimuthal angle), and the event was recorded if any jet E_T exceeded a specified threshold. During the 1994–1995 run, the thresholds were 30, 50, 85, and 115 GeV, with integrated luminosities of 0.353 ± 0.027, 4.69 ± 0.37, 54.7 ± 3.4, and 91.9 ± 5.6 pb^{-1}, respectively [8]. The luminosities of the 30 and 50 GeV triggers were determined by matching their dijet cross sections to that measured for the 85 GeV trigger. This resulted in an additional uncertainty of 4.9% in the luminosities of the 30 and 50 GeV triggers.

Jets were reconstructed offline using an iterative jet cone algorithm with $\mathcal{R} = 0.7$ [9]. Jet E_T is defined as the sum of the E_T in each cell within the cone. The jet was centered on the E_T-weighted pseudorapidity and azimuth of the jet. The jet E_T and direction were then recalculated until the cone direction was stable.

A significant fraction of the data was taken at high instantaneous luminosity, which resulted in more than one $\overline{p}p$ interaction in a beam crossing leading to an ambiguity in selecting the primary event vertex. After event reconstruction, the two vertices with the largest track multiplicity were retained. The quantity $S_T = |\Sigma \vec{E}_T^{\,\text{jet}}|$ was calculated for both vertices, and the vertex with the smaller S_T was selected. The uncertainty on the mass spectrum due to the choice of vertex was 2%. The vertex was required to be within 50 cm of the detector center. This cutoff was $90 \pm 1\%$ efficient, independent of M.

Backgrounds from noise, cosmic rays, and accelerator losses were reduced to an insignificant level by applying jet quality criteria. For an event to be accepted, the two leading-E_T jets were required to satisfy these criteria. Contamination from backgrounds was $<2\%$ based on Monte Carlo simulations and visual inspection of events with high mass. The overall jet selection efficiency for the mass spectrum for $|\eta| \leq 1.0$ was measured as a function of M, giving $93 \pm 1\%$ ($89 \pm 1\%$) at 209 (873) GeV/c^2.

The transverse energy of each jet was corrected for the underlying event, additional interactions, calorimeter noise, the fraction of particle energy that showered hadronically outside of the cone, and for the hadronic response [10]. At $\eta = 0$, the mean total jet energy correction was 16% (12%) at 100 GeV (400 GeV); the correction uncertainty was less than 2.5% of the jet E_T.

For each event that passed the criteria, the dijet mass M was calculated, assuming that the jets are massless, using $M^2 = 2E_T^{\text{jet1}} E_T^{\text{jet2}}[\cosh(\Delta\eta) - \cos(\Delta\phi)]$.

The steeply falling dijet mass spectrum is distorted by jet energy resolution (and to a negligible extent by η resolution). The dijet mass resolution was calculated using the measured single-jet resolutions and the PYTHIA [11] Monte Carlo event generator. This resolution depends on the E_T and η distributions of the two leading E_T jets in each event and is $6.4 \pm 0.7\%$ ($3.8 \pm 0.8\%$) at 200 (1000) GeV/c^2. The observed mass spectrum was corrected with an ansatz function $F(M') = BM'^{-\alpha}[1 - (M'/\sqrt{s})]^{-\beta}$ convoluted with the mass resolutions, to obtain the smeared ansatz $f(M) = \int_0^\infty F(M')\rho(M' - M, M')\,dM'$ (where ρ is the mass resolution), such that the number of events in

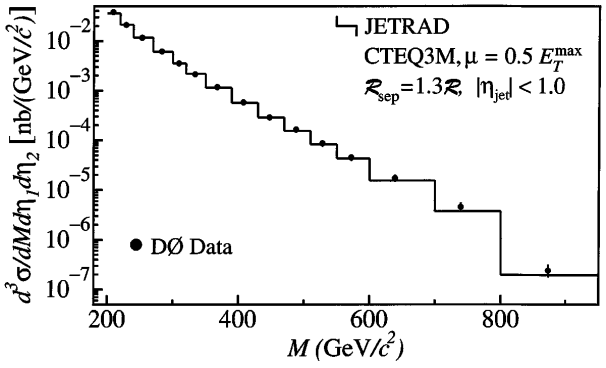

FIG. 1. $d^3\sigma/dMd\eta_1 d\eta_2$ for $|\eta_{\text{jet}}| < 1.0$. The D0 data are shown by the solid circles, with error bars representing the $\pm 1\sigma$ statistical and systematic uncertainties added in quadrature (in most cases smaller than the symbol). The histogram represents the JETRAD prediction.

TABLE I. Dijet cross section for $|\eta_{\rm jet}| < 1.0$ and the ratio $\kappa(|\eta_{\rm jet}| < 0.5)/\kappa(0.5 < |\eta_{\rm jet}| < 1.0)$. High (low) systematic uncertainties are the sum in quadrature of the uncertainties from the $\pm 1\sigma$ variations in the energy calibration, the unsmearing, the vertex corrections, luminosity matching, jet selection, and the uncertainty in the luminosity.

Mass bin (GeV/c^2)				$d^3\sigma/dMd\eta_1 d\eta_2$			Ratio of Mass Spectra
Bin	Min.	Max.	Weighted center	$\pm$ Stat. error (nb)	Syst. low (%)	Syst. high (%)	$\kappa(\lvert\eta_{\rm jet}\rvert < 0.5)/\kappa(0.5 < \lvert\eta_{\rm jet}\rvert < 1.0)$ ($\pm$ stat. error $\pm$ syst. error)
1	200	220	209.1	$(3.78 \pm 0.12) \times 10^{-2}$	-11.4	$+11.8$	$0.613 \pm 0.039 \pm 0.037$
2	220	240	229.2	$(2.10 \pm 0.09) \times 10^{-2}$	-11.3	$+11.6$	$0.614 \pm 0.050 \pm 0.030$
3	240	270	253.3	$(1.16 \pm 0.06) \times 10^{-2}$	-11.5	$+11.7$	$0.570 \pm 0.051 \pm 0.029$
4	270	300	283.4	$(6.18 \pm 0.11) \times 10^{-3}$	-11.5	$+12.0$	$0.568 \pm 0.030 \pm 0.027$
5	300	320	309.3	$(3.55 \pm 0.11) \times 10^{-3}$	-11.5	$+12.1$	$0.610 \pm 0.034 \pm 0.050$
6	320	350	333.6	$(2.12 \pm 0.07) \times 10^{-3}$	-11.9	$+12.3$	$0.705 \pm 0.044 \pm 0.058$
7	350	390	367.6	$(1.18 \pm 0.01) \times 10^{-3}$	-11.1	$+11.6$	$0.672 \pm 0.020 \pm 0.032$
8	390	430	407.8	$(5.84 \pm 0.09) \times 10^{-4}$	-11.5	$+12.2$	$0.593 \pm 0.022 \pm 0.030$
9	430	470	447.9	$(2.89 \pm 0.06) \times 10^{-4}$	-11.9	$+12.9$	$0.708 \pm 0.036 \pm 0.037$
10	470	510	488.0	$(1.64 \pm 0.05) \times 10^{-4}$	-12.4	$+13.5$	$0.690 \pm 0.046 \pm 0.036$
11	510	550	528.0	$(8.74 \pm 0.34) \times 10^{-5}$	-12.8	$+14.3$	$0.620 \pm 0.058 \pm 0.033$
12	550	600	572.0	$(4.49 \pm 0.17) \times 10^{-5}$	-13.5	$+15.3$	$0.634 \pm 0.065 \pm 0.033$
13	600	700	638.9	$(1.73 \pm 0.07) \times 10^{-5}$	-14.9	$+17.2$	$0.647 \pm 0.074 \pm 0.034$
14	700	800	739.2	$(4.58 \pm 0.38) \times 10^{-6}$	-17.6	$+20.8$	$0.608 \pm 0.141 \pm 0.035$
15	800	1400	873.2	$(2.39 \pm 0.35) \times 10^{-7}$	-23.2	$+28.9$	$0.705 \pm 0.246 \pm 0.046$

any given mass bin i is given by integrating f over that bin. The data were then fitted using a binned maximum likelihood method and the MINUIT [12] package to determine the values of B, α, and β ($\chi^2 = 10.8$ for 12 degrees of freedom). The unsmearing correction for each mass bin is then given by $C_i = \int F dM / \int f dM$ [$C_i = 0.96$ (0.92) at 209 (873) GeV/c^2].

The dijet mass spectrum was calculated using $\kappa \equiv d^3\sigma/dMd\eta_1 d\eta_2 = (N_i C_i)/(\mathcal{L}_i \epsilon \Delta M \Delta\eta_1 \Delta\eta_2)$, where N_i is the number of events, $\mathcal{L}_i$ is the luminosity, ϵ is the efficiency of the vertex selection and jet quality cuts, ΔM is the width of the mass bin, and $\Delta\eta_{1,2}$ is the width of the η bin for jets 1 and 2. The spectrum was calculated for the pseudorapidity range $|\eta_{\rm jet}| < 1.0$ (both jets are required to satisfy the η requirement), in mass ranges starting at 200, 270, 350, and 550 GeV/c^2, corresponding to jet E_T thresholds of 30, 50, 85, and 115 GeV.

The cross section for the mass spectrum is plotted in Fig. 1 and given in Table I. The data are plotted at the mass-weighted average of the fit function for each bin ($\int MF dM / \int F dM$). The systematic uncertainties are dominated by the uncertainties due to the jet energy scale, which are 7% (30%) for the 209 (873) GeV/c^2 mass bins. The other uncertainties are due to the luminosity measurement (6.1%), luminosity matching at low mass (4.9%), the unsmearing correction 0.5% (3%) at 209 (873) GeV/c^2, the vertex cut (1%), and the jet selection cuts (1%). The total systematic uncertainty is given by the sum of the individual uncertainties in quadrature. The bin-to-bin correlations of the uncertainties are shown in Fig. 2 [13].

The histogram in Fig. 1 is a prediction for the inclusive dijet mass spectrum from the next-to-leading (NLO) parton level event generator JETRAD [14]. The NLO calculation requires specification of the renormalization and factorization scales ($\mu = 0.5 E_T^{\rm max}$, where $E_T^{\rm max}$ is the maximum jet E_T in the generated event), pdf (CTEQ3M [15]), and parton clustering algorithms. Two partons are combined if they are within $\mathcal{R}_{\rm sep} = 1.3\mathcal{R}$, as motivated by the separation of jets in the data [9]. Choosing an alternative pdf (CTEQ4M [15], CTEQ4HJ [15], or MRS(A′) [16]) alters the prediction by as much as 25%, and varying μ in the range $0.25 E_T^{\rm max}$ to $2E_T^{\rm max}$ alters the normalization by up to 30% with some M dependence. The CTEQ3M and MRS(A′) pdf's are fits to collider and fixed target data sets published before 1994. CTEQ4M updates these fits using data published before 1996, and CTEQ4HJ adjusts the gluon distributions to fit the CDF inclusive jet cross section measurement [2]. Figure 3 shows the ratio (data-theory)/theory for the JETRAD prediction using CTEQ3M

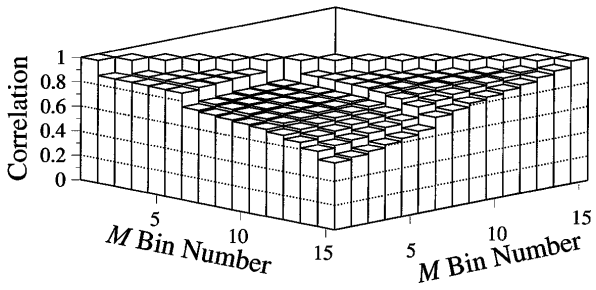

FIG. 2. The correlations between systematic uncertainties in bins of dijet mass (see Table I) for $|\eta_{\rm jet}| < 1.0$. The correlations are calculated using the average systematic uncertainty. The discontinuities arise from the uncorrelated errors (adjacent to correlations of 1.0) and luminosity matching.

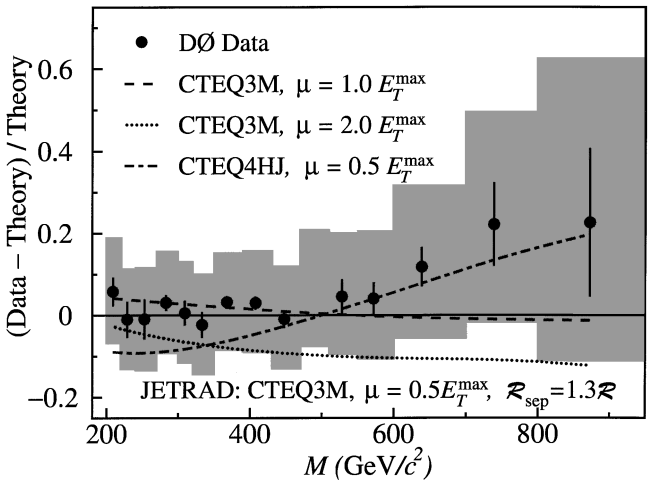

FIG. 3. The difference between the data and the prediction (JETRAD) divided by the prediction for $|\eta_{\text{jet}}| < 1.0$. The solid circles represent the comparison to the calculation using CTEQ3M with $\mu = 0.5E_T^{\max}$. The shaded region represents the $\pm 1\sigma$ systematic uncertainties. The effects of changing the renormalization scale and choosing a different pdf are also shown (each curve shows the difference between the alternative prediction and the standard prediction).

with $\mu = 0.5E_T^{\max}$. Given the experimental and theoretical uncertainties, the predictions can be regarded as in good agreement with the data. The data are also in agreement within the given uncertainties with the cross section measured by CDF [6].

In Table II, we show the χ^2 resulting from a fit of theory to our data, using the full correlation matrix between different mass bins. The choice of pdf and renormalization scale is varied; all choices give reasonable probability.

The ratio $\kappa(|\eta_{\text{jet}}| < 0.5)/\kappa(0.5 < |\eta_{\text{jet}}| < 1.0)$, given in Fig. 4 and Table I, exploits the high correlation between uncertainties in the measurement of the dijet mass spectrum. The resulting cancellation of uncertainties leads to a systematic error of less than 8% for all M. The uncertainty in the theoretical prediction of this ratio is less than 3% due to the choice of pdf, and 6% from the choice of renormalization and factorization scale (excluding $\mu = 0.25E_T^{\max}$).

TABLE II. χ^2 values calculated for various theoretical predictions for the dijet mass spectrum with $|\eta_{\text{jet}}| < 1.0$ and for the ratio of cross sections (15 degrees of freedom).

pdf	D	Mass spectrum		Ratio	
	where $\mu = DE_T^{\max}$	χ^2	Prob.	χ^2	Prob.
CTEQ3M	0.25	12.2	0.66	40.5	0.00
CTEQ3M	0.50	5.0	0.99	15.9	0.39
CTEQ3M	0.75	5.3	0.99	14.7	0.48
CTEQ3M	1.00	5.4	0.99	14.3	0.51
CTEQ3M	2.00	4.2	1.00	13.7	0.55
CTEQ4M	0.50	4.9	0.99	15.7	0.40
CTEQ4HJ	0.50	5.0	0.99	16.0	0.38
MRS(A′)	0.50	6.3	0.97	16.3	0.36

The χ^2 values are shown in Table II. The predictions are in good agreement with the data, except for $\mu = 0.25E_T^{\max}$ which is excluded by the data.

The ratio of the mass spectra can be used to place limits on quark compositeness. A mass scale Λ characterizes both the strength of the quark-substructure coupling and the physical size of the composite state. Limits are set, assuming that $\Lambda \gg \sqrt{\hat{s}}$ (where $\sqrt{\hat{s}}$ is the center of mass energy of the colliding partons), such that quarks appear to be pointlike. Hence, the substructure coupling can be approximated by a four-Fermi contact interaction giving rise to an effective Lagrangian [1] $\mathcal{L} = A(2\pi/\Lambda^2)(\overline{q}_L\gamma^\mu q_L)(\overline{q}_L\gamma_\mu q_L)$, where $A = \pm 1$, and q_L represents left-handed quarks. Limits are presented for the case where all quarks are composite, showing both constructive interference (Λ^{-1} for $A = -1$) and destructive interference (Λ^{+} for $A = +1$). Currently, there are no NLO compositeness calculations available; therefore, the PYTHIA event generator is used to simulate the effect of compositeness. The ratio of these LO predictions with compositeness to the LO with no compositeness is used to scale the JETRAD NLO prediction, as shown in Fig. 4.

We employ a Bayesian technique [17] to obtain from our data a limit on the scale of compositeness. Motivated by the form of the Lagrangian, a uniform prior is assumed in $\xi = 1/\Lambda^2$, and a Gaussian likelihood function $P \propto e^{-\chi^2/2}$ is used. The 95% confidence limit in Λ is determined by requiring that $\int_0^{\xi} P(\xi')d\xi' = 0.95$. Since the ratio at NLO is sensitive to the choice of μ and pdf, each possible choice is treated as a different theory. The most conservative (CTEQ3M, $\mu = E_T^{\max}$) lower limits on the mass scale at the 95% confidence level are found to be $\Lambda^{+} > 2.7$ TeV and $\Lambda^{-} > 2.4$ TeV. These limits are incompatible with the suggestion of a compositeness scale Λ in the 1.5 to 1.8 TEV range found from earlier measurements [2] of the high E_T jet inclusive cross section.

In conclusion, we have measured the cross section for the inclusive dijet mass spectrum for $|\eta_{\text{jet}}| < 1.0$ with

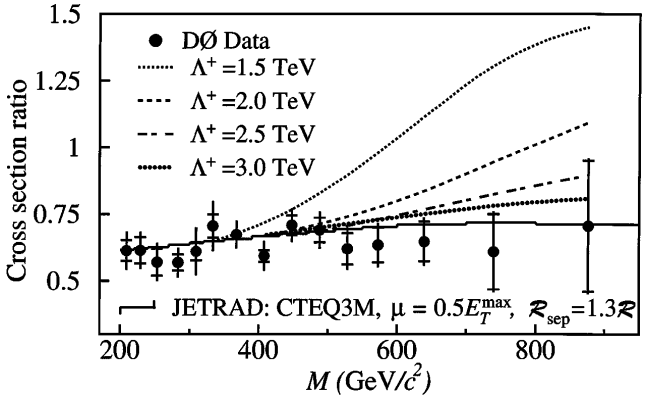

FIG. 4. The ratio of cross sections for $|\eta_{\text{jet}}| < 0.5$ and $0.5 < |\eta_{\text{jet}}| < 1.0$ for data (solid circles) and theory (various lines). The error bars show the statistical and systematic uncertainties added in quadrature, and the crossbar shows the size of the statistical error.

$M > 200\ \mathrm{GeV}/c^2$, and the ratio of cross sections for $|\eta_{\mathrm{jet}}| < 0.5$ and $0.5 < |\eta_{\mathrm{jet}}| < 1.0$, as a function of dijet mass. The data distributions are in good agreement with NLO QCD predictions. Models of quark compositeness with a contact interaction scale of less than 2.4 TeV are excluded at the 95% confidence level.

We thank the staffs at Fermilab and collaborating institutions for their contributions to this work, and acknowledge support from the Department of Energy and National Science Foundation (U.S.A.), Commissariat à L'Energie Atomique (France), State Committee for Science and Technology and Ministry for Atomic Energy (Russia), CAPES and CNPq (Brazil), Departments of Atomic Energy and Science and Education (India), Colciencias (Colombia), CONACyT (Mexico), Ministry of Education and KOSEF (Korea), and CONICET and UBACyT (Argentina). We thank W. T. Giele, E. W. N. Glover, and D. A. Kosower for help with JETRAD.

*Visitor from Universidad San Francisco de Quito, Quito, Ecuador.

†Visitor from IHEP, Beijing, China.

[1] E. Eichten, K. Lane, and M. E. Peskin, Phys. Rev. Lett. **50**, 811 (1983); E. Eichten, I. Hinchcliffe, K. Lane, and C. Quigg, Rev. Mod. Phys. **56**, 579 (1984), Addendum—*ibid.* **58**, 1065 (1986); K. Lane, hep-ph/9605257, 1996.

[2] CDF Collaboration, F. Abe *et al.*, Phys. Rev. Lett. **77**, 438 (1996).

[3] D0 Collaboration, B. Abbott *et al.*, Phys. Rev. Lett. **80**, 666 (1998).

[4] CDF Collaboration, F. Abe *et al.*, Phys. Rev. Lett. **77**, 5336 (1996); *ibid.* **78**, 4307(E) (1997).

[5] D0 Collaboration, B. Abbott *et al.*, preceding Letter, Phys. Rev. Lett. **82**, 2451 (1999).

[6] CDF Collaboration, F. Abe *et al.*, Phys. Rev. D **48**, 998 (1993).

[7] D0 Collaboration, S. Abachi *et al.*, Nucl. Instrum. Methods Phys. Res. Sect. A **338**, 185 (1994).

[8] J. Bantly *et al.*, Report No. Fermilab-TM-1995, 1997.

[9] B. Abbott *et al.*, Report No. Fermilab-Pub-97/242-E.

[10] D0 Collaboration, B. Abbott *et al.*, hep-ex/9805009, Nucl. Instrum. Methods Phys. Res., Sect. A (to be published).

[11] T. Sjöstrand, Comput. Phys. Commun. **82**, 74 (1994). We used PYTHIA version 5.7.

[12] F. James, CERN Program Library Entry D506 (unpublished), We used MINUIT version 96.a.

[13] See AIP Document No. E-PAPS: E-PRLTAO-82-046913 for file with cross sections. E-PAPS document files may be retrieved free of charge from our FTP server (http://www.aip.org/pubservs/paps.html) or from ftp.aip.org in the directory /epaps/. For further information, email: paps@aip.org; or fax: 516-576-2223.

[14] W. T. Giele, E. W. N. Glover, and D. A. Kosower, Nucl. Phys. **B403**, 633 (1993). We used JETRAD version 2.0.

[15] CTEQ Collaboration, H. L. Lai *et al.*, Phys. Rev. D **51**, 4763 (1995); CTEQ Collaboration, H. L. Lai *et al.*, Phys. Rev. D **55**, 1280 (1997).

[16] A. D. Martin, R. G. Roberts, and W. J. Stirling, Phys. Lett. B **354**, 155 (1995).

[17] H. Jeffreys, *Theory of Probability* [Clarendon Press, Oxford, 1939 (revised 1988)], p. 94.